

## Scientific justification

ALMA has made increasingly clear that annular gaps and emission rings are common in the millimeter continuum of protoplanetary disks (e.g. ALMA Partnership et al. 2015, Andrews et al. 2016, Isella et al. 2016, Fedele et al. 2017). The origins of these features are highly debated. Popular hypotheses include planet-disk interactions (e.g. Zhu et al. 2012, Dong et al. 2017), particle trapping (e.g. Pinilla et al. 2012, Ruge et al. 2016), and changes in dust properties near molecular snowlines (e.g., Zhang et al. 2015, Okuzumi et al. 2016, Pinilla et al. 2017). Given the prevalence of these structures, identifying their formation mechanism is key to our general understanding of disk evolution.

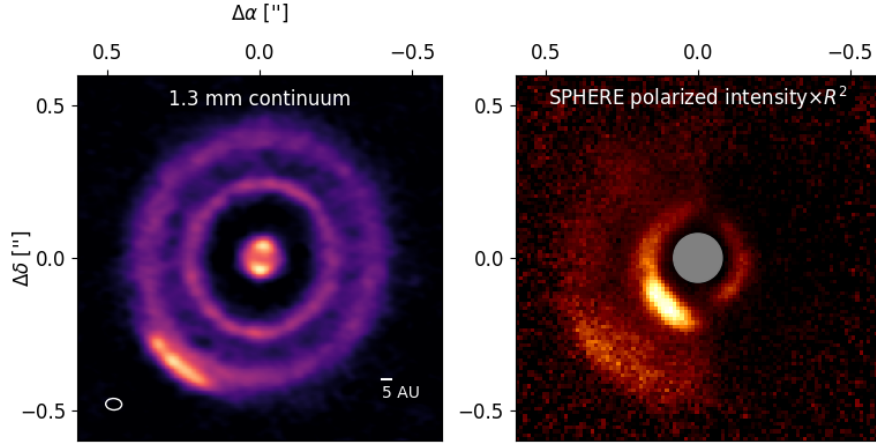


Figure 1: *Left*: 1.3 mm continuum observations of HD 143006 at an angular resolution of 50 mas (8 AU). *Right*: SPHERE polarized intensity image of HD 143006, with a standard  $r^2$  scaling to account for the radial decrease in stellar illumination (Benisty et al. in prep)

One disk exhibiting remarkable substructure is HD 143006, which we observed at a resolution of  $\sim 50$  mas as part of an ALMA Large Program surveying dust substructures in protoplanetary disks (2016.1.00484.L, PI: S. Andrews). We resolve a triple ring system in the 1.3 mm continuum, with the outermost ring featuring a brightness asymmetry in the southeast. Members of our team also obtained SPHERE scattered light observations (Benisty, Juhász, Facchini et al. in prep), revealing emission features that appear to coincide with the outer gap, bright ring, and asymmetric feature seen in the millimeter continuum. In addition, models from Benisty et al. indicate that the brightness asymmetry at  $\sim 0.2''$  in the SPHERE image can be explained by shadowing from an inner disk warp.

## Proposed observations

A key avenue for distinguishing between hypotheses for explaining dust substructures in a protoplanetary disk is to measure its gas surface density profile. For example, in addition to creating dust gaps and vortices, massive planets are expected to carve annular gas gaps depleted up to three orders of magnitude (e.g. Zhu et al. 2011, Pinilla et al. 2012, Fung et al. 2014). While MHD models indicate that millimeter gaps and gas surface density perturbations may instead occur near dead zone edges in disks, they also predict featureless scattered light images and extremely elongated vortices (Régaly et al. 2013, Flock et al. 2016), which do not match well with the existing data for HD 143006 (Fig. 1). Finally, while molecular snowlines may create concentric features in the dust distribution, they are not expected to perturb the gas distribution (Pinilla et al. 2017). **Hence, to investigate whether planet-disk interactions are responsible for the dust substructures around HD 143006, we propose high angular resolution observations of  $^{13}\text{CO } J = 2 - 1$  to trace the gas surface density profile of the disk and to assess its correspondence with the features observed in millimeter continuum emission and scattered light.**

HD 143006 presents one of the best opportunities to elucidate the mechanisms creating complex dust substructures. First, it exhibits bright CO isotopologue emission free of cloud contamination (see Fig. 2), which is not the case for a large fraction of disks. For example, in our ALMA Large Program surveying 20 disks, most of our sources feature gap and ring structures, but the majority also exhibit cloud contamination that would impede efforts to characterize the gas distribution through observations of CO isotopologues, the best gas tracer accessible with ALMA (e.g. Molyarova 2017). We emphasize that even though disks with multi-ringed dust structures may well be nearly ubiquitous, opportunities to measure their gas surface densities are comparatively rare. Hence, case studies of disks like HD 143006 are critical for interpreting the characteristics of the general population.

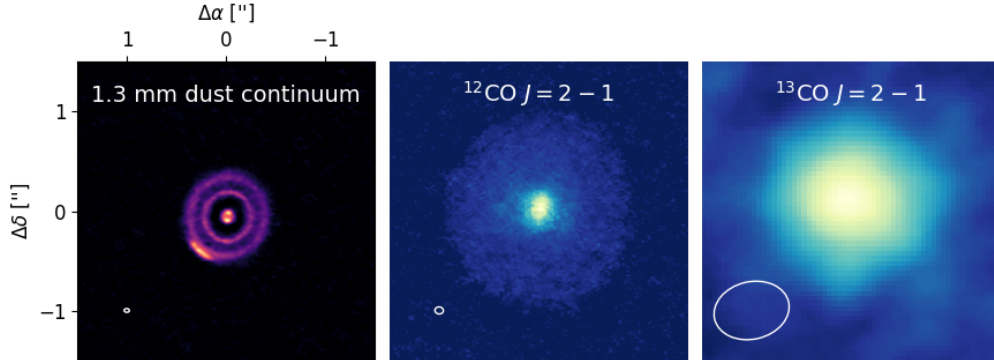


Figure 2: *Left*: ALMA Large Program observations of the 1.3 mm continuum of HD 143006. *Middle*: ALMA Large Program observations of  $^{12}\text{CO}$   $J=2-1$ . *Right*: ALMA observations of  $^{13}\text{CO}$   $J=2-1$  at  $0.7''$  resolution (program 2015.1.00964.S).

Second, the radial locations of the substructures are particularly well-suited to tracing gas with  $^{13}\text{CO}$ . Adopting a distance of 166 pc (Gaia Collaboration et al. 2016), the two millimeter gaps are centered at  $R \sim 25$  and  $\sim 52$  AU, and the outermost emission ring peaks at  $R = 70$  AU. Because HD 143006 is a G7 star (Luhman and Mamajek 2012), its disk should be relatively warm—radiative transfer models of the SPHERE observations of HD 143006 indicate that the midplane does not reach typical CO freezeout temperatures ( $\sim 20$  K) until  $R = 75$  AU (Benisty et al. in prep), placing the dust gaps well interior to the expected location of the CO snowline. Hence, the gas surface density profile we derive in the region traced by the millimeter continuum emission should be robust against assumptions about CO freezeout. This advantage is particularly important for identifying gas gaps given that the CO snowline may create an annular gap in CO emission that could be difficult to distinguish from a gap in the underlying gas (e.g. Schwarz et al. 2016).

We select  $^{13}\text{CO}$  to trace gas surface density because of the high optical depth of the main isotopologue,  $^{12}\text{CO}$ . Observations of  $^{12}\text{CO}$  from the Large Program appear to be largely smooth (Fig. 2), but they demonstrate the feasibility of imaging spectral lines at high resolution. We target the  $J = 2 - 1$  transition of  $^{13}\text{CO}$  because we have a flux measurement from ALMA at  $0.7''$  resolution, anchoring our estimate of the necessary integration time to observe the line at higher resolution. While  $\text{C}^{18}\text{O}$  has lower optical depth than  $^{13}\text{CO}$ , we determined that it would likely be impractical to image at high resolution in the HD 143006 disk based on the flux of previous  $0.7''$  ALMA observations of the  $J = 2 - 1$  line (2015.1.00964.S, PI: K. Öberg).

Sensitivity to the effects of Jupiter-mass planets is of special interest given their hypothesized role in creating vortices that result in millimeter continuum asymmetries like that observed in HD 143006 (e.g. Li et al. 2005, Fu et al. 2014). Simulations from Pinilla et al. (2012) indicate that a  $1 M_{\text{Jup}}$  planet can create a gas surface density drop ranging from one to three orders of magnitude, depending on the disk viscosity. Measurements of gas surface density drops in transition disks have ranged from factors of 40 to 10000 (van der Marel et al. 2016, Fedele et al. 2017). We elect to be

conservative and aim to detect a factor of 10 depletion in gas within the millimeter gaps, which sets our required sensitivity at  $1 \text{ mJy beam}^{-1}$  in  $0.5 \text{ km s}^{-1}$  channels.

To estimate the required integration time, we first devised a parametric temperature structure motivated by radiative transfer models of SPHERE observations of HD 143006 (Benisty et al. in prep). We then constructed a  $^{13}\text{CO}$  surface density profile with a 20 AU-wide gap centered at a radius of 25 AU and a 15 AU-wide gap centered at a radius of 52 AU, based on the widths of the gaps observed in millimeter emission. The  $^{13}\text{CO}$  profile was scaled according to the flux of  $^{13}\text{CO } J = 2 - 1$  observed at low resolution and the radial extent of  $^{12}\text{CO}$  at high resolution (Fig. 2), and model line emission cubes were generated with the RADMC3D code. We aim for a resolution of  $\sim 0.06''$  to resolve gas structures on scales comparable to the continuum emission features and a maximum recoverable scale of  $2''$  based on previous CO observations. Our simulations with CASA `simobserve` indicate that we can detect gas gaps depleted by a factor of 10 or higher with a combination of 5.5 hours on source in C43-8 and 1.2 hours in C43-5, requiring a total of 13.6 hours after accounting for overhead (Fig. 3). The observing ratio is in accordance with the Proposer’s Guide.

In addition to our main target,  $^{13}\text{CO}$ , we will observe  $^{12}\text{CO}$  and  $\text{C}^{18}\text{O } J = 2 - 1$  in the same spectral setup. Compared to the Large Program, the integration time is increased by a factor of 4 and the spectral resolution ( $0.1 \text{ km s}^{-1}$ ) is increased by a factor of 6, improving our ability to check  $^{12}\text{CO}$  for thermal asymmetries or twisted velocity fields due to the disk warp inferred from SPHERE (e.g., Facchini et al. 2018). We do not target  $\text{C}^{18}\text{O}$  in the long-baseline observations because we determined that it would be impractical to image at high resolution based on the flux of  $0.7''$  ALMA observations of the  $J = 2 - 1$  line (2015.1.00964.S, PI: K. Öberg); instead we place an additional continuum window to facilitate self-calibration of the spectral lines and to check the relative flux scaling between execution blocks. We include  $\text{C}^{18}\text{O}$  in the compact configuration ( $\sim 0.25''$ ) observations to maximize archival value and as an additional constraint for the inferred CO abundance structure.

## Analysis plan

To derive a gas surface density structure from  $^{13}\text{CO}$  observations, we will first refine our temperature estimate for the disk by fitting the high resolution SPHERE and ALMA continuum data with dust radiative transfer calculations from RADMC3D. We will then test different parametric  $^{13}\text{CO}$  abundance structures (accounting for photodissociation and freezeout) by calculating the corresponding line emission cubes with RADMC3D. We favor the parametric modeling approach described because of the frugality in the number of physical assumptions that have to be made and the efficiency with which degeneracies in the models can be explored (e.g. Isella et al. 2016, Huang et al. 2018). For high angular resolution spectral line observations, special care is required to account for the effects of the  $uv$  coverage and the imaging algorithm on inferred features. Hence, as with our team’s previous analysis of long-baseline  $^{12}\text{CO}$  observations of TW Hya (Huang et al. 2018), we will generate model visibilities at the same  $uv$  points and re-image with the same method used for our data in order to test for artifacts and to provide the fairest comparison to the observations.

Our team was also allocated time with the NaCo instrument on the Very Large Telescope (program 101.C-0466, PI L. Pérez) in the April to September 2018 observing period to image HD 143006 at  $L'$  at a sensitivity sufficient to detect planetary masses of  $1 M_{Jup}$  or higher. The combination of VLT observations and our requested line observations, complemented by existing SPHERE scattered light and ALMA continuum data, will provide key tests of disk simulations:

1. The simultaneous detection of a companion and a gap in  $^{13}\text{CO}$  emission would provide the first direct test of models associating planetary masses with the sizes of gaps carved in disks (e.g. Fung et al. 2014, Duffell et al. 2015, Dong et al. 2017).
2. The detection of a companion without an associated gap in  $^{13}\text{CO}$  emission would indicate that the absence of a deep gas gap does not rule out the presence of a massive companion, suggesting

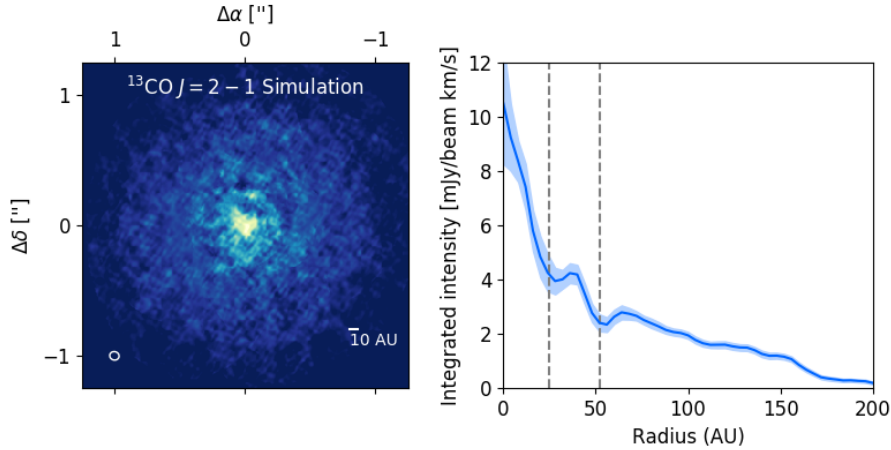


Figure 3: *Left*: Simulated moment 0 map of simulation of  $^{13}\text{CO } J = 2 - 1$  at a resolution of 60 mas. *Right*: Radial profile of  $^{13}\text{CO } J = 2 - 1$  simulation. Vertical lines mark the centers of the two gaps in the input CO model. The shaded region denotes the  $1\sigma$  error, defined as the standard deviation of the pixel intensities divided by the square root of the number of beams within each annulus.

a high disk viscosity and motivating the development of alternative tests to distinguish between dust structure formation scenarios.

3. The detection of a gap in  $^{13}\text{CO}$  emission without a companion would indicate that large gas gaps are not necessarily carved by massive planets, contrary to inferences made from previous disk observations (e.g. van der Marel et al. 2016, Fedele et al. 2017). Although the viscosity of protoplanetary disks remains an open question, models indicate that in highly inviscid disks, it is feasible for a single super-Earth to create concentric double gaps and a vortex, reminiscent of the features observed in HD 143006 (Dong et al. 2017, Bae et al. 2017). On the other hand, if the shape and location of a  $^{13}\text{CO}$  gap has no clear correspondence with the millimeter gaps, this would point to a non-planetary origin.
4. The dual absence of a gap in  $^{13}\text{CO}$  emission and a companion would motivate further exploration of whether the substructures originate from either molecular snowlines or dead zones. In particular, we could use our derived temperature structure to distinguish between these possibilities by checking whether the radial locations of the substructures correspond to any molecular snowlines.

## References

- ALMA Partnership et al. 2015, ApJ, 808, L3  
 Andrews, S. M. et al., 2016, ApJL, 820, L40  
 Bae, J. et al., 2017, ApJ, 850, 201  
 Benisty, M., Juhász, A., Facchini, S. et al., in prep  
 Dong, R. et al., 2017, ApJ, 843, 127  
 Duffell, P.C. et al., 2015, ApJL, 801, L11  
 Facchini, S. et al., 2018, MNRAS, 473, 4459  
 Fedele, D. et al., 2017, A&A, 600, A72  
 Flock, M. et al., 2015, A&A, 574, A68  
 Fu, W. et al. 2014, ApJL, 788, L41  
 Fung, J. et al., 2014, ApJ, 782, 88  
 Gaia Collaboration et al. 2016, A&A, 595, A2  
 Huang, J. et al., 2018, ApJ, 852, 122  
 Li, H. et al. 2005, ApJ, 624, 1003  
 Luhman, K. L. & Mamajek, E. E. 2012, ApJ, 758, 31  
 Molyarova, T. et al. 2017, ApJ, 849, 130  
 Okuzumi, S. et al., 2016, ApJ, 821, 82  
 Pinilla, P. et al., 2012, A&A, 538, 114  
 Pinilla, P. et al., 2017, ApJ, 845, 68  
 Régaly, Z. et al. 2013, MNRAS, 433, 2626  
 Rosenfeld, K.A. et al., 2014, ApJ, 757, 129  
 Ruge, J. P. et al., 2016, A&A, 590, 17  
 Schwarz, K. R. et al. 2016, ApJ, 823, 91  
 van der Marel, N. et al. 2016, A&A, 585, A58  
 Zhang, K. et al. 2015, ApJ, 806, L7  
 Zhu, Z. et al., 2011, ApJ, 729, 47  
 Zhu, Z. et al., 2012, ApJ, 755, 6